SHORTENING OF SOUTHERN TIBET

Sarah McLeod

SUBMITTED IN PARTIAL FULFILLMENT OF THE REQUIREMENTS FOR THE DEGREE OF BACHELOR OF SCIENCES, HONOURS DEPARTMENT OF EARTH SCIENCES DALHOUSIE UNIVERSITY, HALIFAX, NOVA SCOTIA

April 27h, 2018

Distribution License

DalSpace requires agreement to this non-exclusive distribution license before your item can appear on DalSpace.

NON-EXCLUSIVE DISTRIBUTION LICENSE

You (the author(s) or copyright owner) grant to Dalhousie University the non-exclusive right to reproduce and distribute your submission worldwide in any medium.

You agree that Dalhousie University may, without changing the content, reformat the submission for the purpose of preservation.

You also agree that Dalhousie University may keep more than one copy of this submission for purposes of security, back-up and preservation.

You agree that the submission is your original work, and that you have the right to grant the rights contained in this license. You also agree that your submission does not, to the best of your knowledge, infringe upon anyone's copyright.

If the submission contains material for which you do not hold copyright, you agree that you have obtained the unrestricted permission of the copyright owner to grant Dalhousie University the rights required by this license, and that such third-party owned material is clearly identified and acknowledged within the text or content of the submission.

If the submission is based upon work that has been sponsored or supported by an agency or organization other than Dalhousie University, you assert that you have fulfilled any right of review or other obligations required by such contract or agreement.

Dalhousie University will clearly identify your name(s) as the author(s) or owner(s) of the submission, and will not make any alteration to the content of the files that you have submitted.

If you have questions regarding this license please contact the repository manager at dalspace@dal.ca.

Grant the distribution license by signing and dating below.

_____ _____

Name of signatory Date

DALHOUSIE UNIVERSITY

Department of Earth Sciences
Halifax, Nova Scotia
Canada B3H 4R2
(902) 494-2358

DATE: 03/30/2018

AUTHOR: Sarah McLeod

TITLE: Shortening Estimates of Southern Tibet

DEGREE: Earth Sciences CONVOCATION: June YEAR: 2018

Abstract

The Himalayan orogeny began approximately 50 million years ago with the collision of the Indian and Eurasian plates, which caused deformation and uplift of the Himalayas and Tibetan Plateau. As this deformation propagated it deformed lithotectonic units independently allowing us to study the deformation of a specific time. The Tethyan Himalaya lithotectonic unit is a fold-and-thrust belt in southern Tibet between the crest of the Himalaya and the India-Eurasia suture (the Indus-Tsangpo suture Zone) that developed during the Eocene and Oligocene. We know from seafloor data that the rate of Indian plate movement has always been faster in the east than in the west, and that during the Eocene and Oligocene was faster than during Miocene, however, current shortening estimates across the Tethyan Himalaya do not reflect this. There are two principal objectives of this project. The first is to calculate the amount of shortening of the Tethyan Himalaya. Secondly, we aim to determine the geometry of the basal detachment of the Tethyan Himalaya. The current hypothesis is that the basal detachment of this fold-and-thrust belt was a south verging thrust during Eocene and Oligocene, which was reactivated during Miocene as a low angle normal fault shear zone. This structure out crops in the northern Himalaya as the South Tibetan Detachment. The objective of this project is the creation of two cross section template construction using MOVE software to create internally consistent cross sections in order to compare shortening estimates through the Himalayas. The cross sections will be constructed based on published geological maps and field observations. The long-term aim of the project is to determine if there were spatial and temporal changes in the shortening rate of the southern Tibet and the Himalaya.

Key Words: Himalayan Orogeny, Retro deformation, Shortening, Tethyan Sedimentary Sequence

Table of Contents

List of Figures

Acknowledgements

I would like to thank my supervisor Djordje Grujic for the opportunity to explore Himalayan geology. I would also like to thank my honours class for all their support during the year. I could not have made it here with out you guys!

Chapter 1: Introduction

1.1 Overview

The goal of this thesis is to construct several cross sections through the Tethyan Sedimentary Sequence in order to help better define constraints on shortening rates through the Himalayas, specifically in the Tethyan Sedimentary Sequence. Due to time constraints and complexity of the sections, two cross section templates were completed using Midland Valley's MOVE software.

In an established orogenic zone such as the Himalayas the deformation rate is dependant on the plate convergence if all other erosional and accretionary processes are in equilibrium (Hilley and Strecker, 2004). The deformation rate is dependant on the plate convergence rates the amount of deformation can be estimated through time based on known plate convergence rates found from seafloor data. The paleo convergence rates collected from seafloor data show an uneven convergence rate throughout the last 50 Ma suggesting that the deformation recorded in the Himalayan rocks should reflect the same uneven deformation rates as convergence rates.

1.2 Purpose of Project

Presently there is only one study which estimates the amount of shortening in the Tethayn Himalaya which was done over 20 years ago by hand. This study aims to create a balanced cross section that can be used to estimate the amount of shortening during the Oligocene and Eocene when the Tethyan Sedimentary Sequence was being deformed. The reconstruction of these balanced cross sections using the same software as other researchers would create internally consistent data that would be able to be used in larger scale Himalayan studies.

Chapter 2: Geological Setting

2.1 Geology of the Himalayas

The Himalayan mountain range and Tibetan plateau formed from the collision of the Eurasian and Indian plate. The collision of these two plates which began approximately 50 million years ago caused deformation as well as uplift of the Himalaya and Tibetan plateau to average 5 Km elevation (Le Fort, 1975; Royden et al, 2008). The Himalayan mountains form a 250km by 2500km wide arc running on the southern margin of the Tibetan plateau (Le Fort, 1975). The Tibetan plateau is approximately 3 million km^2. The Tibet and Himalayan collision zone is large orogenic zone that represents of approximately 1000km of shortening (Murphy and Yin, 2005).

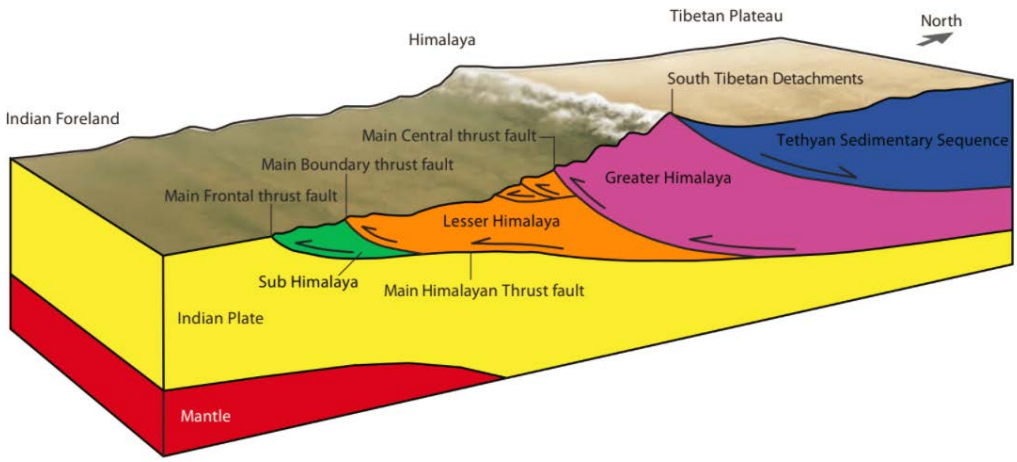

Figure 2.1- Schematic Cross section of the Himalayan Orogen showing lithotectonic units and bounding structures. From Hirschmiller, 2013

2.1.1 Lithotectonic Units

The Himalayas are comprised of four distinct lithotectonic units each representing distinct depositional environments and deformation history.

2.1.1.1 Tethyan Sedimentary Sequence

The Tethyan Sedimentary Sequence (TSS) consists of a relatively complete stratigraphic section of the Indian continental shelf. The base of TSS is not exposed so the oldest age of the

lithotectonitc unit is unknown (Hodges, 2000; Rowly, 1996). The lowest exposed unit in TSS represents a pre-rift sequence of Proterozoic to Devonian marine sediments transiting from shallow to deep marine (Godin et al, 2003; Hodges, 2000). During the Carboniferous to Lower Jurassic carbonate platforms were deposited from the rift sequence which created the Neo-tethy ocean (Godin et al, 2003). As Gondwana began to breakup siliciclastic transgressive regression system tracts were deposited on the passive continental margin from the Jurassic to Cretaceous (Aikman et al, 2008. Hodges, 2000). Finally, from Cretaceous to Eocene syn-collisional sediments have been deposited (Gordin et al, 2003).

The TSS was deformed during the Middle Eocene to Late Oligocene which represents the collision of India and Eurasia (Aikman, 2008; Hodges, 2000). The exact timing of the initial collision is highly debated but generally agreed to be around 54-50Ma based on transitions from marine to non-marine sediments and the K-Ar age of a synkinematic muscovite (Rowley, 1996. Hodges, 2000. Ratsbacher et al, 1994). The deformation of the TSS is progressively younger from north to south and have corresponding changing geometries (Hodges, 2000). In the north folds are upright and reverse faults are steeply dipping to the north (Ratschnacher et al, 1994. Hodges, 2000). In the middle portion of TSS both folds and faults have shallower dipping axial planes and dips respectively (Ratschnacher et al, 1994). In the south folds and faults are in classic ramp-flat-ramp geometries of a fold and thrust belt (Hodges, 2000).

2.1.1.2 Greater Himalaya Sequence

The Greater Himalaya Sequence (GHS) is considered the metamorphic core of the Himalayas as it is a highly metamorphosed zone of both metasedimentary and meta-igneous rocks. The GHS can be divided into two structural levels. The lower structural level is a volcano-sedimentary unit deposited in Cambrian to Ordovician time and has undergone middle to upper amphibolite facies metamorphism to create the present orthogneiss unit (Rowley, 1996). The upper structural unit is a metasedimentary unit deposited from Neoproterozoic to Ordovician as siliciclastic and calcareous rocks (Long et al, 2011. Hodges, 2000). Peak metamorphism and deformation for all of GHS occurred in Early to Middle Miocene (Long et al, 2011). Based on garnet-biotite temperature estimates the lower structural unit reached approximately 500^{o}C deformation temperature and the upper structural unit reached approximately 670^{o}C (Larson and

Gordin, 2009). The main driver of metamorphism in the GHS is crustal thickening causing Barrovain-type metamorphism (Larson and Gordin, 2009).

2.1.1.3 The Lesser Himalayan Sequence

The Lesser Himalayan Sequence (LHS) is fold and thrust belt consisting of tight, overturned folds duplexes which dip towards the hinterland (Mitra et al, 2010. Hodges, 2000). The deformation of the LHS occurred between approximately 12-5 Ma (DeCelles et al, 2001). The LHS does not have an exposed basement but is assumed have been deposited on the Indian passive margin (Hodges, 2000). The lower portion of the rock succession is dominated by siliciclastic rocks and in the upper succession the rocks are more dominated by carbonate and siliciclastic rocks (DeCelles et al, 2001). These rocks exhibit a small amount of low grade greenschist metamorphism due to deformation estimated at approximately 350^{o}C (Célérier et al, 2009).

2.1.1.4 Sub-Himalaya Sequence

The Sub-Himalaya Sequence (SHS) is an active tectonic wedge at the southern edge of the Himalayas (Husson et al, 2004). It is a fold and thrust belt made up of synorogenic Siwlik Group rocks which are Neogene to Quaternary succession of coarsening upward conglomerate, sandstone, and siltstone (Husson et al, 2004. Célérier et al, 2009. DeCelles et al, 2001). These rocks have been deformed by faulting which activated in the Pliocene, resulting in north dipping bedding (DeCelles et al, 2001).

2.1.2 Bounding Structures

Each of the lithotectonic units have distinct structural boundaries separating them. The bounding structures generally began deforming in the north and propagated southward with time (DeCelles et al, 2001).

2.1.2.1 Indus-Tsangpo Suture

The Indus-Tsangpo Suture Zone represents the collision zone between the Indian and Eurasian plates (Hodges, 2000). This suture is a south dipping, north verging thrust that places the accreted block of the Himalayan orogeny rocks on top of the Indian subcontinent (Xu et al, 2015. Murphy et al, 2002). It contains four distinct components from the two colliding plates that

have been sutured together to from the Indus Tsangpo Zone including the Transhimalayan components, Neo-Tethyan Ocean floor components, Indian plate components and Indus-Tsanpgo Suture Zone Allochthons (Xu et al, 2015. Hodges, 2000).

The Transhimalayan component has been interpreted to be a forearch sequence deposited to the south of the continental arc composed of Middle Cretaceous turbidites. The Neo-Tethyan Ocean-Floor components are Jurassic to Cretaceous deep ocean sediments and ophiolites (Xu et al, 2015). The oceanic sediments were metamorphosed from low temperature deformation most commonly to green schist facies. The Indian plate components are the sediments representing the Indian shelf and slope deposits characterized by Triassic-Cretaceous tributes (Hodge, 2000).

2.1.2.2 South Tibetan Detachment System

The South Tibetan detachment system is an east striking extensional fault system (Wiesmayr et al, 2002. Hodges, 2000). This system separates the relatively unmetamorphosed rocks of the Tibetan zone from the lower Greater Himalaya zone (Hodges, 2000). The faulting of the south Tibetan detachment system shows top to north shear strain and consists of normal faults which are traceable throughout most of the Himalayan strike zone (Murphy et al, 2002. Murphy and Yin, 2003).

2.1.2.3 Main Central Thrust System

The GHS is thrust on to the LHS by the Main Central Thrust (MCT) which is a broad ductile shear zone resulting in a top-to-the-south detachment (Larson and Gordin, 2009). The MCT was active in the Miocene (DeCelles et al, 2001).

2.1.2.4 Main boundary thrust system

The boundary between the LHS and SHS are the north dipping faults of the main boundary thrust system (Hodges, 2000). This thrust system places the LHS on top of the SHS by moderate to steeply dipping thrust faults (Wiesmayr et al, 2002). The Main Boundary Thrust became active approximately 5 Ma (DeCelles et al, 2001).

2.1.2.5 Main Frontal Thrust System

The Main Frontal Thrust System (MFT) deforms that Siwalik group for the SHS (DeCelles et al, 2001). As this thrust system cuts through Quaternary conglomerates the fault system is approximately 3 Ma (DeCelles et al, 2001).

2.2 Tethyan Sedimentary Sequence

2.2.1 Lithology

The TSS contains a relativity continuous stratigraphic record from the Indian continental margin during the Paleozoic to Eocene (Garzanti, 1999. Hodges, 2000). The thickness of the TSS is unknown as the base of the section is not exposed (Hodges, 2000). The lowest most stratigraphic unit sits above the high grade metamorphic rocks which belong to the GHS (Hodges, 2000). This oldest unit exposed are Lower Cambrian aged shallow marine sediments which have been heavily metamorphosed (Garzanti, 1999. Hodges, 2000). These shallow marine sediments prograde upward into deep marine dolomitic sediments deposited during the Upper Cambrian Epoch (Garzanti, 1999. Hodges, 2000). The breakup of Gondwana caused the development of the Neo-Tethys Ocean in the Permian which deposited interbedded sandstone and mudstones (Garzanti, 1999). Based on biostratigraphy of these beds the interbedded sandstone and mudstone was deposited in the Upper Carboniferous to Lower Permian (Garzanti, 1999). At the top of the Neothetheyan Oceanic sediments there is basaltic lava flows believed to be due to Neo-Tethyan seafloor spreading (Garzanti, 1999). Costal and shallow marine pelagic carbonate deposits continued until from the Permian into the Triassic when there was a global sea level rise (Garzanti, 1999. Hodges, 2000). The sediments from the Jurassic and Cretaceous periods record transgressive and regressive periods (Garzanti, 1999. Hodges, 2000). Finally, in the late Cretaceous the sediment becomes more clastic with sporadic alkaline volcanics. This marks the Indian plate detaching from Gondwana and beginning its move towards the Eurasian plate (Garzanti, 1999. Hodges, 2000).

The sediments of the Tibetan Sedimentary Sequence are relatively unmetamorphosed but within structural horse's low to medium metamorphic assemblages are present (Kawakami et al, 2007). Within the Tibetan sedimentary sequence there is a band of gneiss domes called the Northern Himalayan Gneiss domes. These domes are mainly distributed discontinuously

throughout the northern portion of TSS, however, they have also been documented in the Indus-Tsangpo suture zone (Kawakami et al, 2007. Rowley, 1996). The mechanism to place these gneiss domes within unmetamorphposed rocks is unclear however based on $^{40}Ar/^{39}Ar$ biotite dates the emplacement is believed to occurred around 30Ma (Kawakami et al, 2007. Hodges, 2000).

2.2.2 Internal Structure

The TSS is bounded on the southern boundary by a set of normal faults (South Tibetan detachment) believed to be a result of ductile shear zone overprinted by brittle faults (Gordin, 2003. Murphy and Yin, 2003). he TSS is a fold- and- thrust belt unit which was deformed during Eocene and Oligocene to form south directed thrusts and south verging folds (Aikman et al, 2008. Hodges, 2000). The general shape of folding changes from the north to south through the TSS with steeply dipping north moving reverse faults in the north and shallowly dipping axial planes of the folds in the south shown in figure 2.2 (Hodges, 2000). The southern folds have classic ramp-flat geometry (Hodges, 2000). Gyirong-Kangmar important thrust in the TSS separating these northern and southern regions (Aikman et al, 2008. Hodges, 2000). The Gangdese Thrust, is a south verging thrust along boundary of Gangdese intrusive rocks (Hodges, 2000).

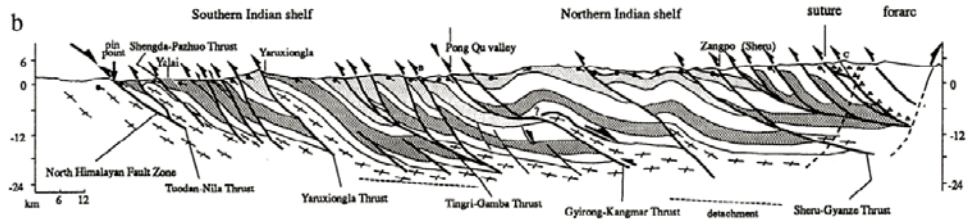

Figure 2.2. Cross Section of TSS from Ratschbacher et al 1994 showing the shape of folding and thrusting in the TSS as well as highlighting important folds

Current estimates of shortening due to folding and in the TSS between the South Tibetan detachment and the Indus Tsangpo Suture is 67% (Ratschbacher et al, 1994).

2.3 Fold and Thrust Belts

2.3.1 Critical Coulomb Wedge

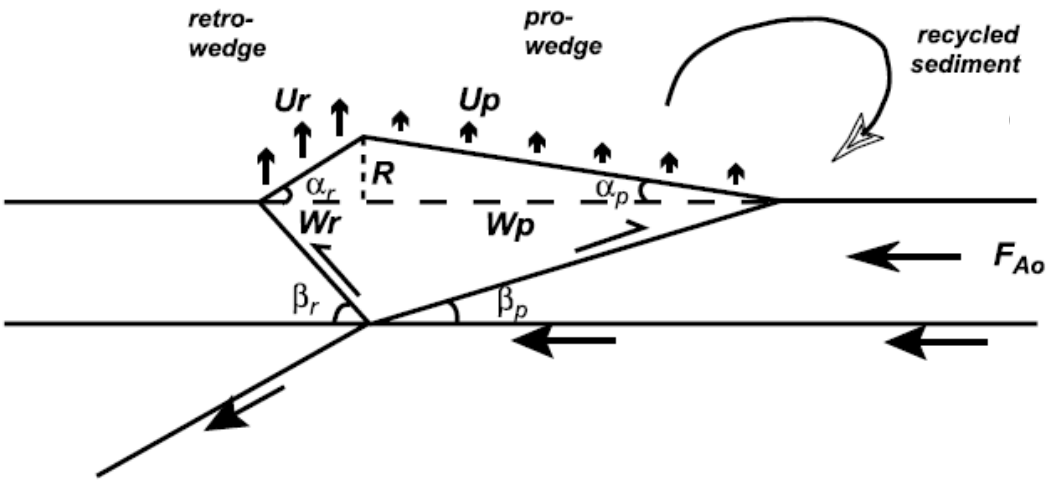

Figure 2.3. Diagram of Critical Coulomb Wedge Geometry indicating Retro-wedge and Pro-wedge. From Whipple and Meade, 2004

An accretionary prism and fold and thrust belt are defined by the basal detachment and the angle to its surface with its slope. Together the dip of the basal detachment (β) and the surface slope (φ) define the angle of the wedge (Whipple and Meade, 2004).

$$\text{Equation 1 } \alpha + \beta = \varphi_{b-}\varphi_o$$

This is called the critical taper because it is assumed that the stresses in the wedge are in balance, the yield stress allowing the wedge to glide along the basal detachment (Dahlen, 1990). The shape of this wedge is dependent on the relationship between the tectonics processes imputing material and the erosional processes acting on the wedge. Their dynamic relation is defined by the Mohr-Coulomb criteria (equation 1). The basic shape of the wedge has the upper surface dipping the opposite way of the detachment. This configuration is what creates the wedge shape seen in figure 2.3. The relative angle of the bounding surfaces of the wedge are determined by the relationship between the rate accretion of material to the rate and amount of surface erosion (Whipple and Meade, 2004). If the mechanical parameters are in equilibrium the geometric parameters remain in constant equilibrium with each other (Dahlen, 1990).For example, if there is too much accretion of material to the wedge, the upper slope will steepen and trigger more

erosion to remove rock and maintain the slope angle, or the wedge will propagate into the foreland (ad a new tectonic slice) therefore reducing the angle of the wedge. In contrast if there is too much erosion the angle will get bellow the critical taper, to compensate the deformation will jump back into the wedge and trigger out-of-sequence thrusting.

The shape of accretionary prism is controlled by the Coulomb failure limit which is a result of the balance between the accretion and erosional process. This balance between accretion and erosion is reached when the Coulomb failure limit is reached. The size of the wedge builds up as much as possible due to accretion of material and erosion removes any material that moves above the failure limit. As the ratio of mass flux over erosion increases so does the width of the acceleration prism (Dahlen 1990; Hilley and Strecker, 2004). The more material that is added to the system causes the slope wedges upper surface to increase (Hilley, 2004). Similarly, as the ratio of material flux due to accretion compared to erosion decreases the over all wedge angle and width of the wedge will decrease (Hilley, 2004).

The geometry of the wedge can be divided into two dependent angles, α and β seen in *figure 2.4*. α describes the angle from the ellipsoid to the upper surface of the wedge and β represents the angle from the ellipsoid to the detachment. The sum total of the α and β remain constant within changes to the accretion and erosion relationship however changes in erosion or accretion can alter the size of α and β (Hilley, 2004).

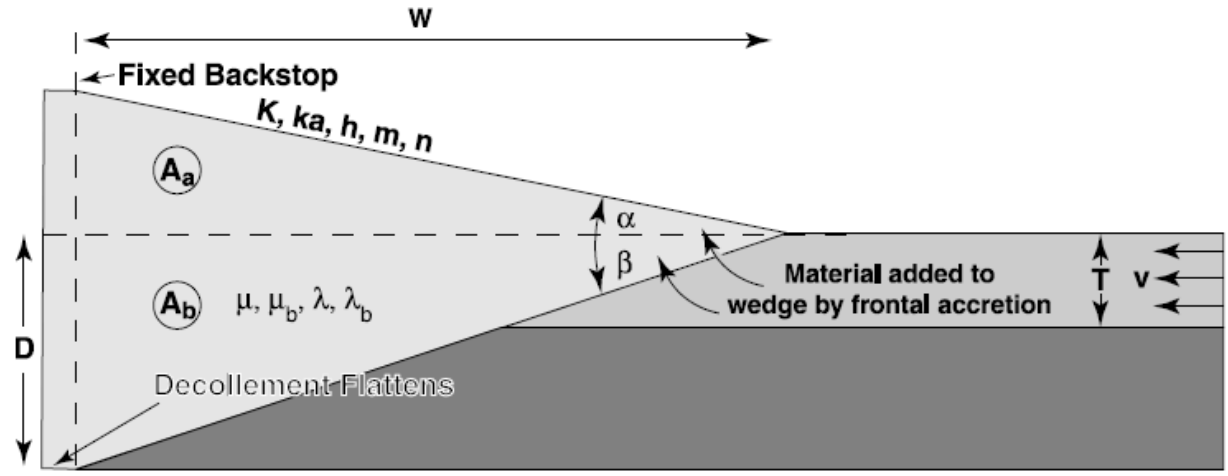

Figure 2.4 Schematic diagram of an Critical Coulomb wedge depicting wedge angles (α and β), wedge thickness (T and D), wedge length (W) and acting forces (V= accretion, K= rock erodibility) From Hilley and Strecker, 2004

2.3.2 Controls of Coulomb Wedge

2.3.2.1 Accretion

The formation of Critical Coulomb Wedge is a balancing act between the surface erosion and accretion of material. Accretion adds material to the toe of the wedge over time. Tectonic rates control amount of accretion (Hilley, 2004). When the density of the material being added to the wedge does not change the accretionary flux (A) of material being added is equal to the product of velocity (v) of the plate convergence and the thickness (T) of the material being added (Dahlen 1990, Whipple et al., 1999; Hilley, 2004). This material can be added to the back of the wedge by thrust propagation (r), or directly to the foreland toe of the wedge (f) (Hilley, 2004).

$$\textit{Equitation 2 } A = vT$$

$$\textit{Equation 3 } vT = v_f T_f + v_r T_r$$

When erosion does not balance the amount of material added to the wedge through accretion it causes the wedge to grow in size (Hilley, 2004). This growth means that the upper slope of the wedge (angle α) increase with the material addition but the overall angle of the wedge (α +β) will remain constant as there has been no change in stresses. The wedge will proportionally widen as more material is added to the system however angles α and β will remain constant (Hilley, 2004).

2.3.2.2 Erosion

If erosion rate (E) increases over a wedge it will remove more material which lowers the angle of the upper slope. In order to maintain the force balance state of the critical Coulomb wedge, the same amount of material that has been accreted to the critical Coulomb wedge must be eroded by surface processes.

$$Equation\ 4\ E = CW(\tan\alpha)^{\beta}$$

Where W= wedge width, and C=coefficient of erosional efficiency

Erosional rates are very effected by climate (Whipple and Meade, 2004). For example, if the change in climate lowers the precipitation, it will lower the rock erodibility which is controlled by channel slope, discharge, and rock erodibility (Hilley, 2004). Channel slope creates a positive feedback loop of erosion. The steeper the slope the more erosion will occur, and as erosion increases it incises deeper river valleys creating an increase in slope (Hilley, 2004). Rock erodibility is dependent on lithology; e.g., high for weakly cemented clastic rocks, low for granite. The erodibility can be also altered due to a change in climate which affects the amount of precipitation eroding the rocks (Hilley and Strecker, 2004).

In a closed system where the width and accretionary flux of the wedge are fixed, erosion is the dominant cause of rock uplift. As in this case the erosion lowers the weight of the over laying rocks resulting in the rocks lifting up (Whipple and Meade, 2004). During steady state of the wedge, erosion is equal to rock uplift (Whipple and Meade, 2004). Orogenic scale erosion is dependent on the topographic gradient and the wedge width (Whipple and Meade, 2004).

2.4 Plate Convergence

2.4.1 Deformation Propagation

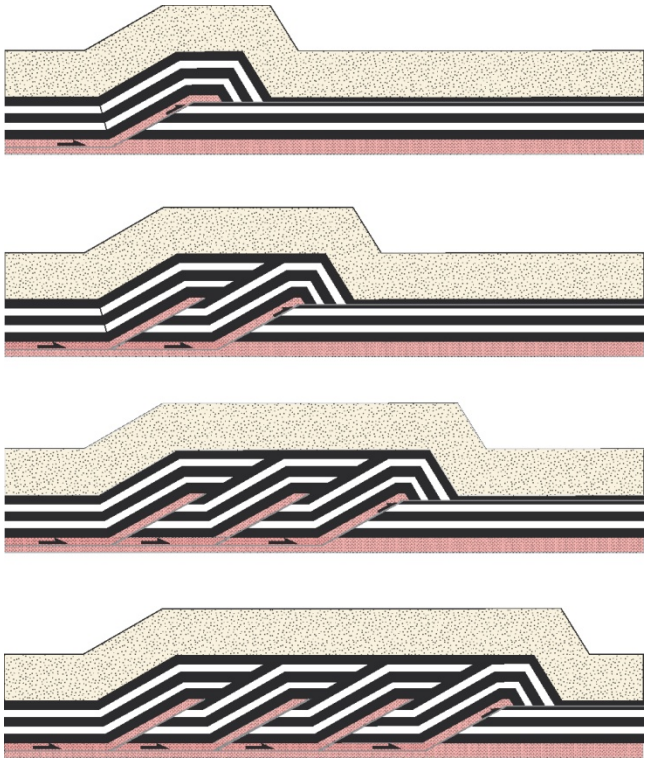

Figure 2.5. Block Diagram showing how deformation propagates from one structural horse to another. From Fossen, 2016

Deformation to the Himalayas did not affect the entire Himalayan area at one time, instead the deformation propagated through each lithotectonic unit through time (Hodges, 2000). The deformation propagated through each of the lithotectionic units at a different time beginning in the North and moving south (Larson et al, 2009). The Himalayas is comprised of a large horse structure which transfers the deformation stresses from one horse to another as the fault plane underthrust the next lithotectonic unit (figure 2.5) (Fossen, 2016). Based on field data and cross cutting relationships of deformation indicators the timing of deformation in each of the lithotectonic units is well constrained (DeCelles et al, 2001). Knowing the timing of deformation in each unit enables the examination of rates, style, and amount deformation of a particular time.

Fault Propagation fold

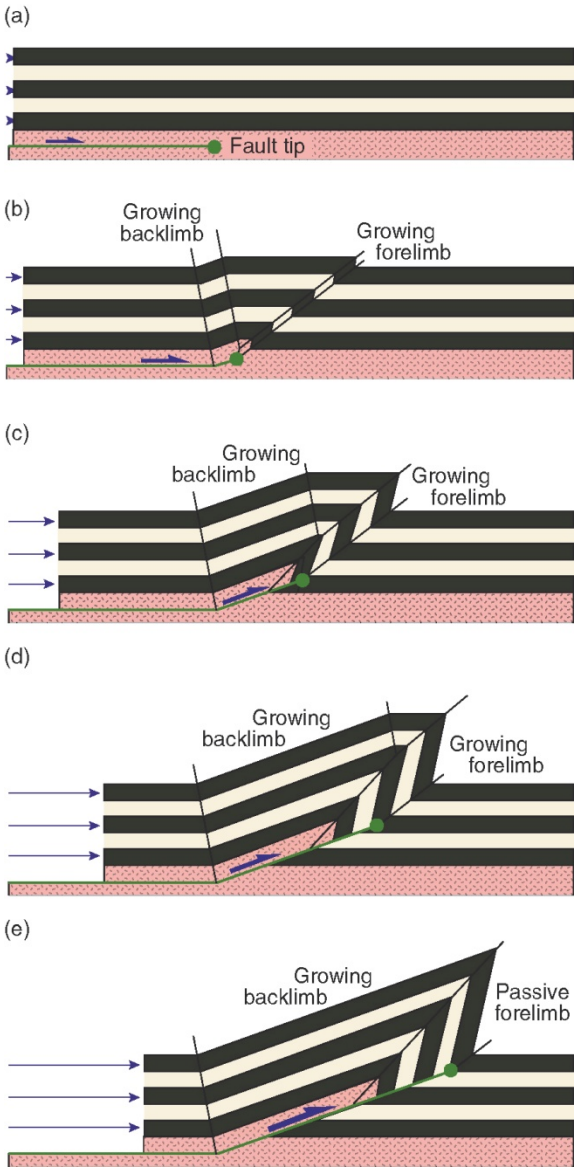

Figure 2.6 Diagram of Fault Propagation Fold causing overturned folds. From Fossen, 2016

Fault propagation folds are the result of a thrust fault deforming a ductile area. In a fault propagation fold the thrust acts on the ramp of the fold beneath the surface and pushed the overriding layers to fold (Fossen, 2016). The resulting folds are often steep, overturned folds seen in figure 2.6. When the fault breaks the surface is projects through the syncline of the overturned fold.

2.4.2 Plate Convergence Rates

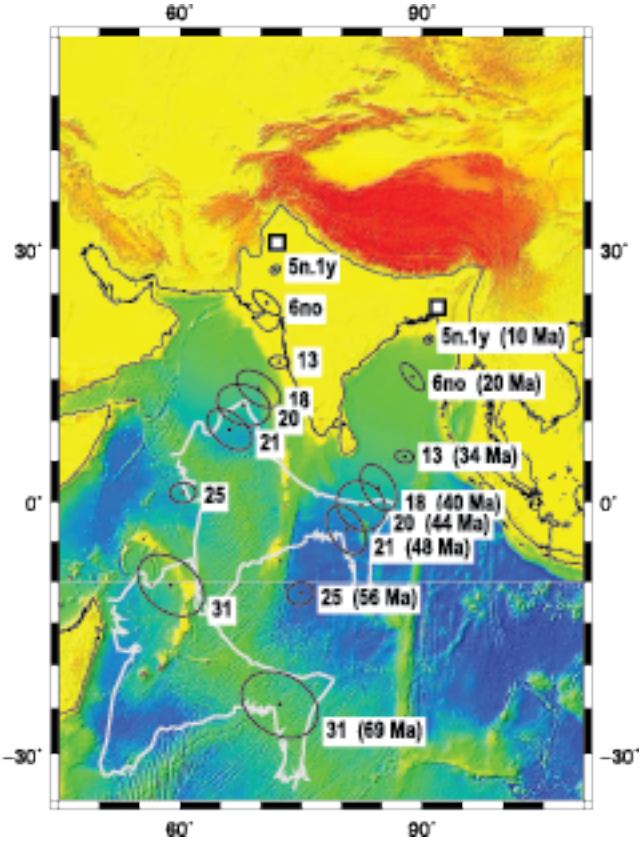

Figure 2.7 Map of convergence rates of the Indian plate converging with the Eurasian plate based on seafloor data. From Molnar and Stock, 2009

Sea floor data has preserved magnetic anomalies that allow for the reconstruction of the spreading rates of the Indian plate as it collided with Eurasia (figure 2.7)(Molnar and Stock, 2009). As the Indian plate moved across the ocean floor it rotated into the Eurasian plate resulting in a quicker plate convergence in the western side of the plate then the east (Molnar and Stock, 2009). The sea floor data recorded the convergence rates throughout the Himalayan orogeny which show the western side of the plate consistently moving quicker than the east. There is also an overall trend of a slowing convergence starting at the timing of collision around 50 Ma and continuing to slow throughout the orogeny (figure 2.8). As the timing of deformation is known in each lithotectonic unit the convergence rate can be correlated to each individual unit. With each lithotectonic unit deformation the rate of plate convergence decreases. The timing of the convergence rates decreases correspond to the timing of the beginning of the deformation of each lithotectonic unit.

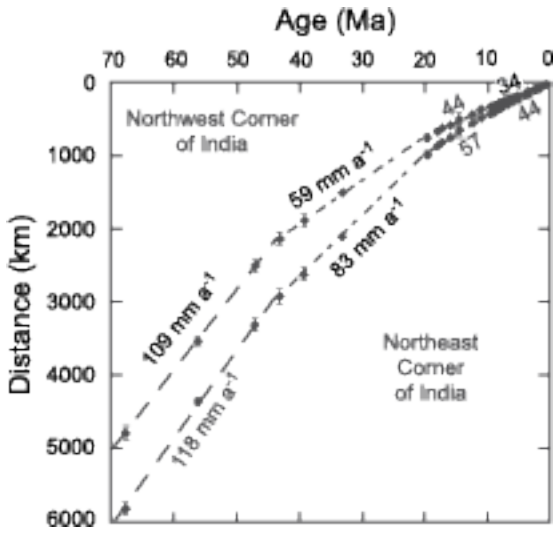

Figure 2.8 Graph of plate convergence rate versus time for the western and eastern corners of the Indian Plate as it collided with Eurasian Plate. From Molnar and Stock, 2009

2.4.3 Existing Estimates

The TSS and LHS have very similar deformation styles, however based on plate convergence rates the amount and intensity of deformation is significantly different. The TSS was deformed for approximately 30 Ma at a rate of 59 mm/a in the west and 88mm/a on the east. The LHS was deformed for approximately 12 Ma at a rate of 34 mm/a on the west and 44mm/a on the east. This data shows that the TSS was deformed for more 50% longer than LHS at over 50%. Therefore, the deformation of the TSS would be predicted to be at least 50% more than the LHS.

The convergence rate of the tectonic plates is the main factor controlling deformation as the accretion and erosion of the Himalayan orogenic wedge is in equilibrium (See earlier chapter). Therefore, based on the paleoconvergence rates there should be more deformation on the western side of the Himalayan orogeny as the convergence rates are consistently quicker on the west than east throughout time. Similarly, the length of time that each lithotectonic unit was deformed for is not constant indicating that the units which were deformed for longer should have show significantly more deformation.

Chapter 3: Methods

3.1 Basic Cross Section Theory

Balancing a cross section adjusts the geologic profile in order to account for both geologic and tectonic controls of the unit's structure. This process requires making assumptions to allow the cross section to be admissible to geologic laws in both its restored and unrestored state.

From a balanced cross section, the original geometry of the units can be restored in order to estimate the amount of deformation that occurred to the units by working backward through each deformation event (Woodward, 1989). This transformation is generally not a linear reconstruction and includes length and area-based calculations (Fossen, 2016). The restoration process does not necessarily need to be restored in order of events but can be restored based types of deformation, like fault offset or folding. The final product of a restored section will have no fault offsets, folded layers or rotated sections and no gaps or overlaps (Woodward, 1989). As assumptions are needed to be implemented in order to balance the section with our gaps or overlap the final balanced section will not necessarily be the true original geometry but based on geologic structure rules is will accurately represent the initial geometry (Woodward, 1989).

3.2 Line Restoration

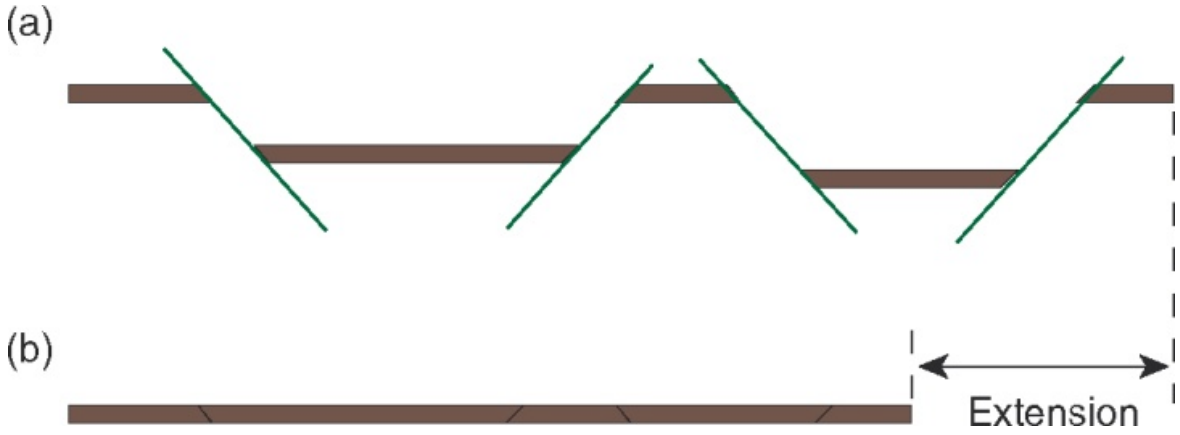

Figure 3.1. Diagram showing how line restoration restores a cross section along faults from the faults in (a) to the restored line in (b). From Fossen, 2016

Line restoration of a cross section is a one-dimensional technique that determines where the straight line was located before it was deformed. Line restoration is based on the assumption that deformation occurred in a 2-D plane where there is no competition or lateral movement in and out of the section (Woodward et al, 1989). In order to restore the line a stratigraphic marker needs to be identified throughout the section to perform the reconstruction. The stratigraphic marker is then moved systematically back into a complete straight line along faults as seen in figure 3.1 (Fossen, 2016). In order to correctly retro deform a one-dimensional section knowing the fault geometry is important to accurately reconstruct the movement of the stratigraphic marker (Woodward et al, 1989). A common marker is a cut offline which is the intersection between a liner feature such as a bed with the fault surface. A good cutoff line is distinguishable in both the hanging wall and foot wall which allows for the fault to be reconstructed to connect the two cutoff lines (Woodard et al, 1989). This method works best with layers that have constant bed thickness as it allows the bed to be easily traced and the deformation force is assumed to be in one direction (Fossen, 2016). An assumption made when using the line restoration method is that the deformation is plane strain as line restoration only examines deformation in one plane of 3-D space. If deformation occurred in more than one direction the line restoration method would be lacking deformation information about the other directions. In

general, ductile strain causes curved lines which need 3-D restoration methods to be accurately restored (Fossen, 2016).

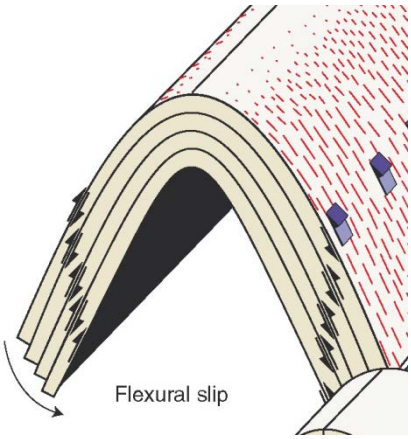

Figure 3.2. Example of how indicate slip plans of a flexural fold remain parallel to one another during deformation. From Fossen, 2016

If the line lengths remain constant the area of the layers will also remain constant. Flexural slip is a common mechanism of folding that preserves both length and area by concentration deformation along the interface of layers (see figure 3.2) (Fossen, 2016).

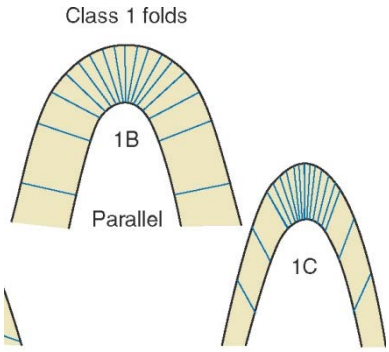

Figure 3.3. Class 1B folds showing flexural folding. Class 1C showing an over tightened 1B fold where more deformation occurs in the hinge than limbs. From Fossen, 2016

When using constant line length to determine the original length of a fold it is important to consider the shape of the fold. When folds are tightly and steeply folded like in the case of overturned folds the layers do not remain parallel (flexural slip) which violates the constant length assumption of constant area (Fossen, 2016). This is show in figure 3.3 where class 1B fold

show even deformation of both the inside and outside edge of the fold through both the hinge and limbs. Where as fold 1C is a tighter fold such as in an overturned fold which no longer has parallel curvature of the inside and outside edges of the fold (Fossen, 2016).

3.3 Area Restoration

Similar to line restoration, area restoration is based on the assumption that deformation occurred in a 2-D plane where there is no competition or lateral movement in and out of the section (Woodward et al, 1989). During deformation the line length is not always preserved, but the area of the deformed rocks will remain constant. If deformation causes a a rock to move out of one area by some vvolume, then the rock must move to another area by the same amount as seen in figure 3.4 where area A equals area B despite a change in layer length (Woodward, 1989). Calculating this area balance can allow for a deformation reconstruction of rocks that have been deformed by more than plane strain.

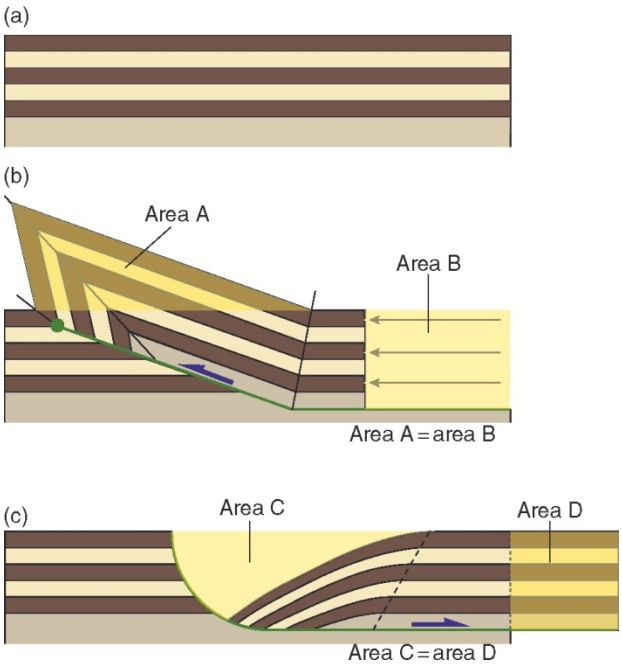

Figure 3.4. Block diagram showing constant area restoration of a cross section. From Fossen, 2016

3.4 Cross Section Workflow

The main source of data for both cross section templates is from the Jiangzi Geologic map created in 2002 by Wenchan et al found in Appendix A. The first step in making the cross-section templates is to digitize this geologic. The digitized geologic boundaries and structural measurements are then imported into MOVE by Midland Valley along with digital elevation (DEM) model of the region. Next an optimal cross section trace is determined based on axial planes of associated fold structures.

After a cross section trace is determined structural measurements and stratigraphy is projected to the cross section. The stratigraphy is manipulated by dip markers to line up the geological layers to their corresponding surface intersection along the trace of surface elevation. At the same time faults are added in to the section. Moving the dips and stratigraphy is an iterative process that takes time to determine a combination that satisfies all geological constraints.

Once a satisfactory cross section is created the software can retro deform the cross section and estimate the amount of shortening within the section. In the case of this study satisfactory cross sections were not achieved but two templates were made and retro deformed using this method.

3.5 Assumptions

The software used to create the cross sections of the area was selected because it is the same software being used to construct shortening estimates throughout the Himalayas. This software is a powerful tool to construct and retro deform a cross section however it is not user friendly when it comes to more advanced structures causing the process of the cross section to be delayed. As a result of the delay a true geologically correct cross section was not achieved, instead a cross-section template was constructed with several simplifications in order to be able to estimate a minimum amount of shortening.

The main assumption made during the construction of the cross sections is there are no over turned folds. The western most cross section has several overturned folds that were to difficult to accurately model in the time given so they have all been modeled as simple synclines

and anticlines. Similarly, small branching faults are throughout the section that have been ignored in order to simplify the model.

Chapter 4: Results

4.1 Balanced Cross Section Templates

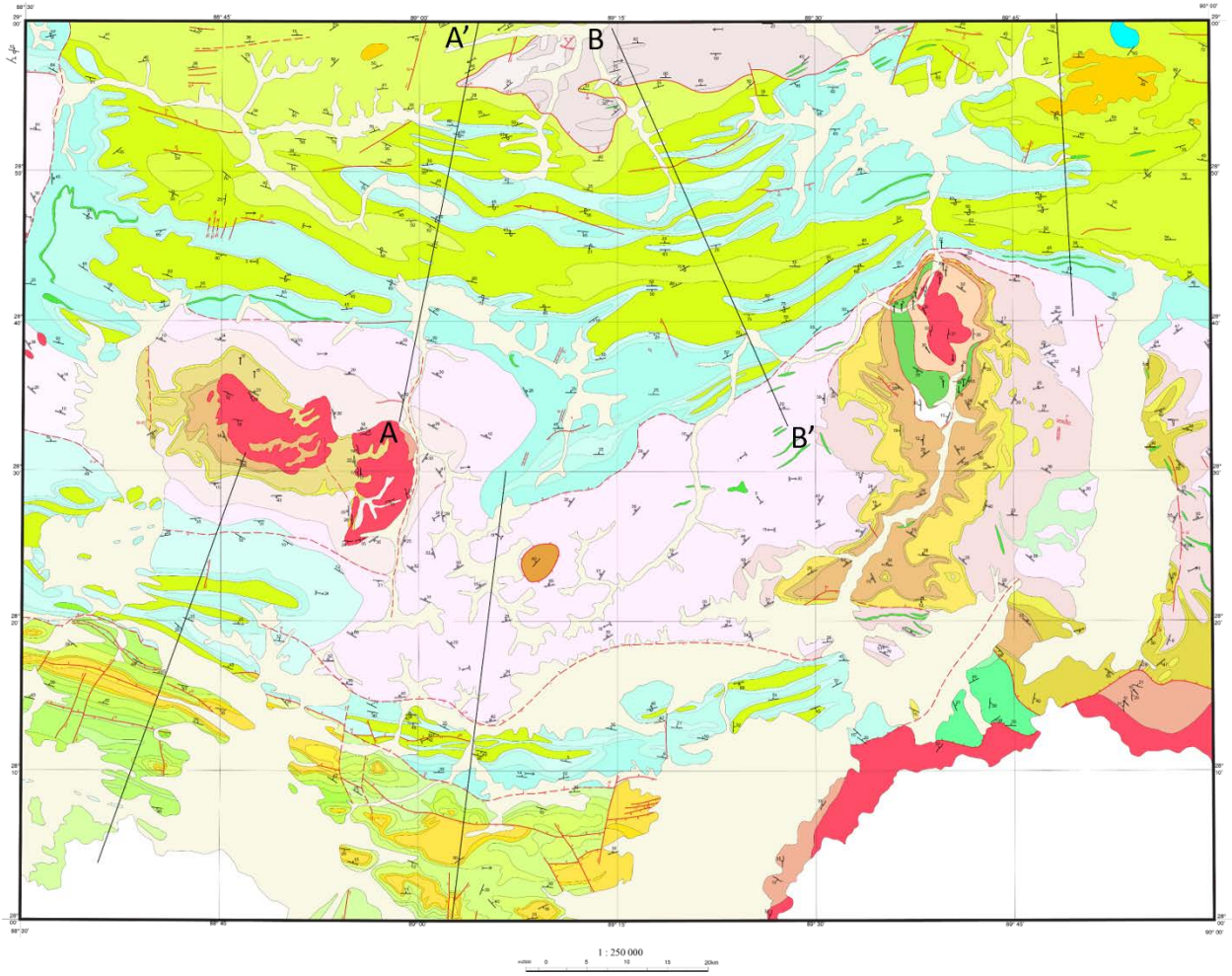

Figure 4.1. Geologic Map of study area showing trace of cross section A, A' and B, B' templates. After Wenchan et al, 2001

Two balanced cross section templates were constructed based on the Jiangzi geologic map (map found in appendix A). The trace of the two cross section templates are shown on the digitized version of the Jiangzi Geologic map in figure 4.1. Due to time, information, and

software constraints many assumptions were made in order to complete these templates. As a result of these assumptions the templates provided are not accurate geological cross sections but instead a starting point for further shortening studies in the area. Based on the templates made a minimum shortening has been estimated for both templates.

The software used to create the cross sections of the area was selected because it is the same software being used to construct shortening estimates throughout the Himalayas. This software is a powerful tool to construct and retro deform a cross section however it is not user friendly when it comes to more advanced structures causing the process of the cross section to be delayed. As a result of the delay in the cross-section construction several simplifications were made in order to be able to estimate a minimum amount of shortening.

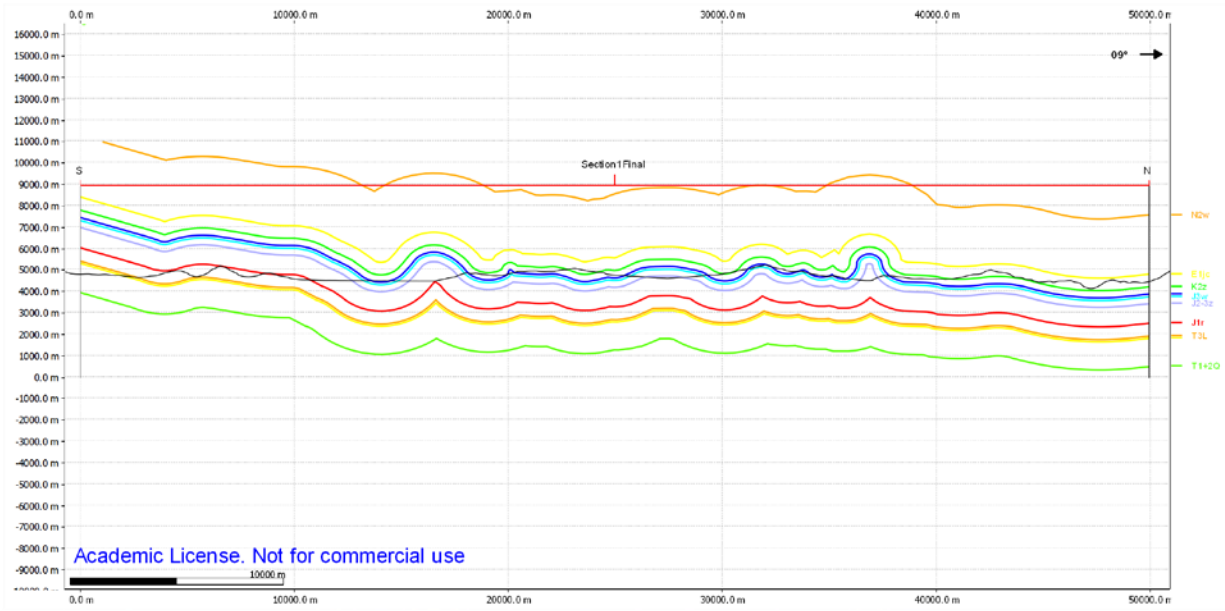

Figure 4.2 Cross Section Template A. Cross section template indicated by A, A' on Figure 4.1

Cross section template A has an overall trend dipping to the north with south verging overturned folds that are modeled here as upright folds. In cross section template A all faulting indicated on the geologic map in the section was not modeled as the faults present are low angled thrusts that only affected a small portion of the template. The cross-section template has a length of 50000 m and based on line restoration methods the average restored length of the units is

53633 m. Therefore, the minimum shortening estimates from cross section template A is 3633 m or 6.77%.

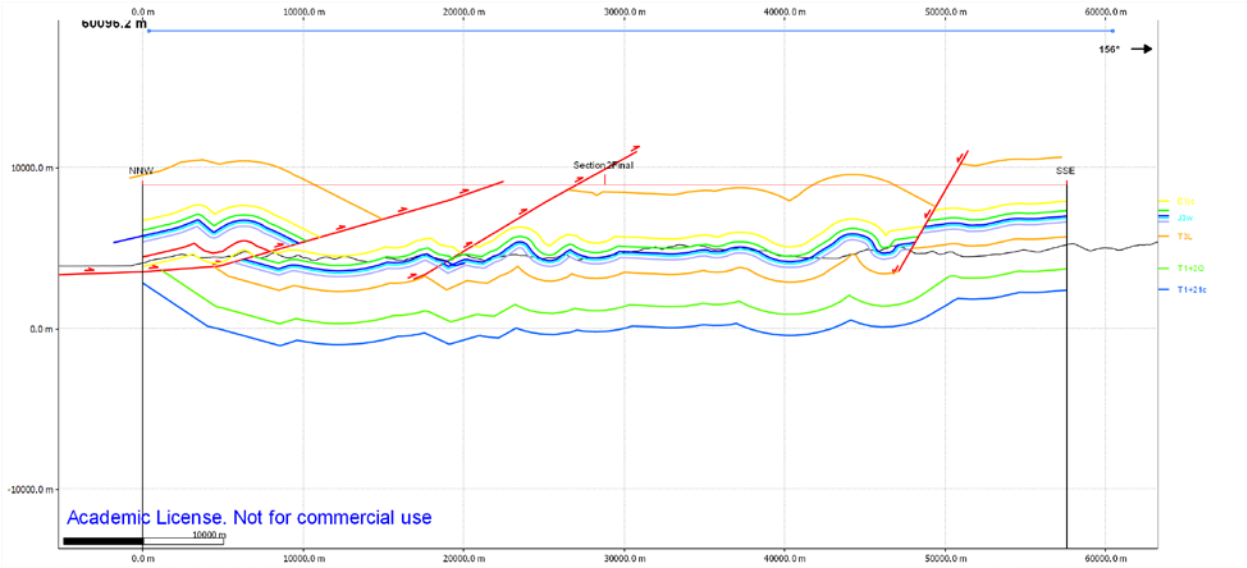

Figure 4.3 Cross Section Template B. Trace of cross section template indicated by B, B' on Figure 4.1

Cross section template B has an overall trend of north dipping stratigraphy which is cross cut by thrust faults that have been interpreted to be low angle thrusts cutting only the Triassic sediments. Some geologic inconsistencies in cross section template B include the southward dip of the lower units in the northern portion of the section template. This southern dip is an artificial result of the modeling process. The length of the cross section template B is 57300 m. This cross section was retro deformed by line restoration method and found an average shortening of 65131 m and 12% shortening.

Chapter 5: Discussion

5.1 Cross Section Template Shape

Cross sections A and B are templates representing the approximate geometry of the structures they are modeling. There are three main reasons why the cross sections are templates. The main reasons these cross sections are templates is complex software that is difficult to use and lack of supporting data to reinforce the models. These factors in combination with the extensive amount of time needed to produce the cross sections have resulted in templates that can be later used to aid in the construction of a more accurate model.

In both cross section templates the most dominant feature is overturned folds which verge to the south. Due to the way the software models the stratigraphy it is extremely difficult to control the shape of an overturned fold. To make a template of the cross sections all of the overturned folds are all modeled as upright folds. Commonly, overturned folds do not have even deformation in their hinges as in their limbs which violates the assumption of constant area in a line restoration method (Woodward et al, 1989). Due to this violation of constant area the line used to retro deform an overturned fold would be longer than in an upright fold. Therefore, modeling the overturned folds as upright folds under estimates the amount of shortening.

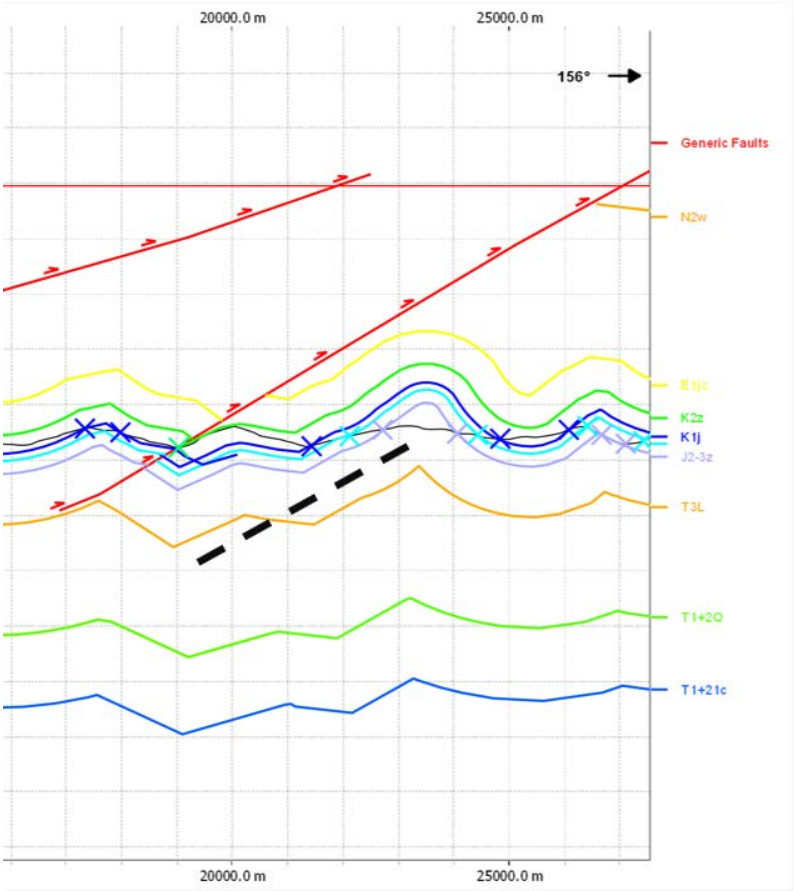

Figure 5.1. Example of over turned fold (modeled as upright) from cross section template B that is likely from a Fault Propagation Fold due to its geometric shape and alignment with the parallel fault. Black dashed line represents possible location of fault.

Shallow fault prorogation is the likely cause of the overturned folds in the cross section templates. This is because there is known faulting in the area, so subsurface faulting would be consistent with the regional geology, as well as the shape of the folds in the cross section templates resemble the geometry of a fault propagation fold. An example is shown in figure 5.1 where a dashed line has been added as an example of where a subsurface fault could lie.

It can not be known if shallow fault propagation is the cause of the overturned folds seen in the cross section templates without more information about the basal detachment. Small scale faults branch off from a main basal detachment, so knowing where the basal detachment is would help determine the placement of the smaller scale folds (Woodward et al, 1989). The faults causing fault propagation folds would project through the synclines of overturned folds

like seen in figure 5.1. Cross section development can also help define the basal detachment geometry by using stratigraphy thickness and structural measurements to determine the shape of the detachment. Both seismic data and constructed cross sections work together to determine the basal detachment. There has been recent seismic studies done in this area that can be used to guide future cross sections. Preliminary results from the seismic data indicates a basal detachment dipping shallowly to the north which agrees with the cross section templates. This agreement of the data indicates a strong

The final shape of the cross section template is dependant on the amount of time it took to construct the section. Digitizing the initial data and importing it into the software as a geographically referenced data took almost a month. Then using the software to construct the cross section took several months to learn how to use the software efficiently to create a cross section. Finally, the supporting seismic data was not processed in order to help constrain the section. Time is the biggest hurtle to creating a balanced cross section. These templates are the result of many months of work towards a balanced cross section that can be used in the further to aid in the creation of a balanced cross section.

5.2 Existing shortening rates

5.2.1 Shortening Throughout the Himalayas

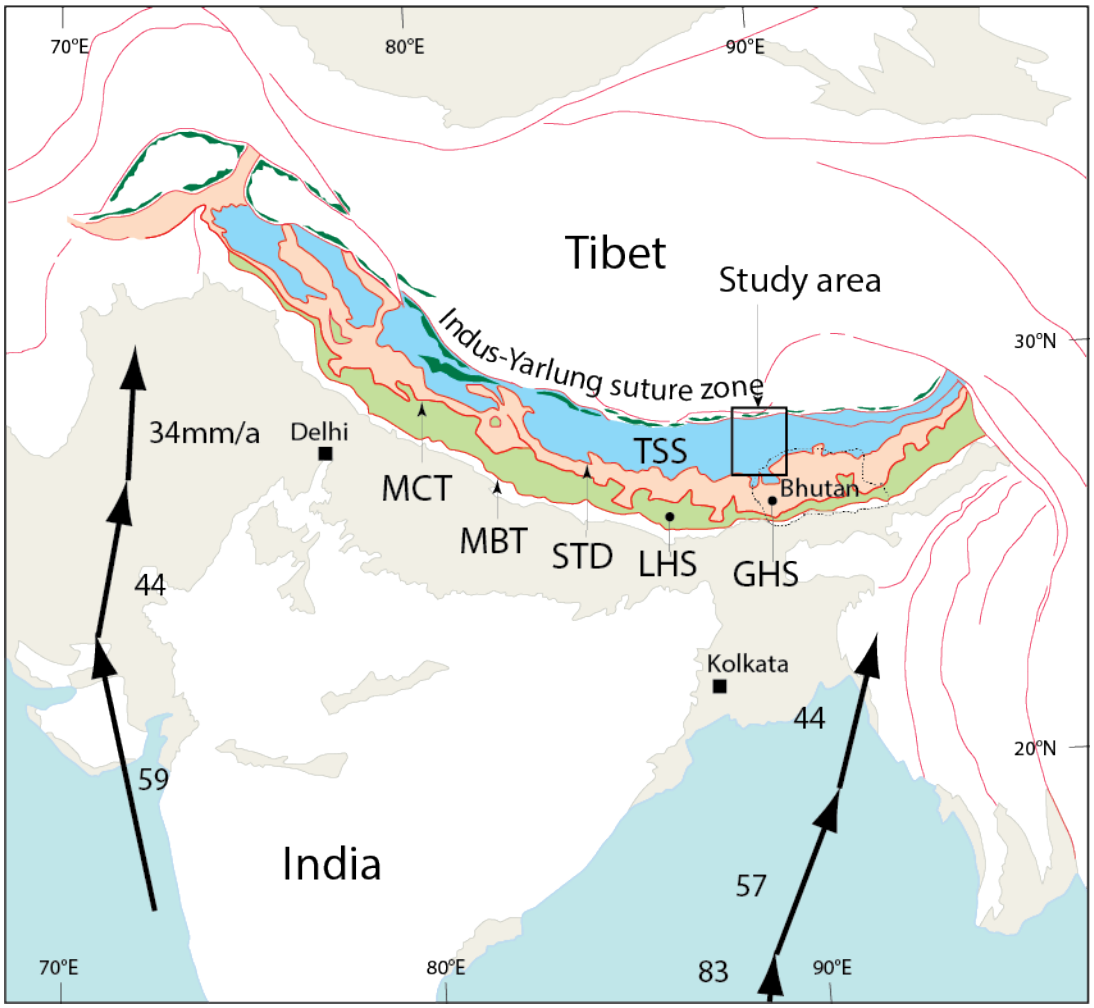

Figure 5.2 Regional map of Himalayas showing lithotectonic units, bounding structures, and rates of plate convergence. From Molnar and Stock, 2009

The convergence rate of the tectonic plates (shown in figure 5.2) is the main factor controlling deformation as the accretion and erosion of the Himalayan orogenic wedge is in equilibrium (Hilley et al, 2004). Therefore, based on the paleoconvergence rates there should be more deformation on the western side of the Himalayan orogeny as the convergence rates are consistently greater on the west than east throughout time. Similarly, the length of time that each lithotectonic unit was deformed for is not constant indicating that the units which were deformed for longer should have show significantly more deformation. Long et al (2011) compiled

shortening estimates for all lithotectocnic units across the Himalayas displayed in figure 5.3. This study shows there is no significant difference in amount of shortening from the northern to southern lithotectonic units and no trend from the west to east of increased shortening rates. Based on the longer deformation period and rater convergence rates it is expected that the TSS has at least twice as much deformation than the similar deformed LHS which is not seen in regional shortening estimates (Long et al, 2011). There is also no obvious trend of more shortening on the western side compared to the eastern side which was expected based on plate convergence rates.

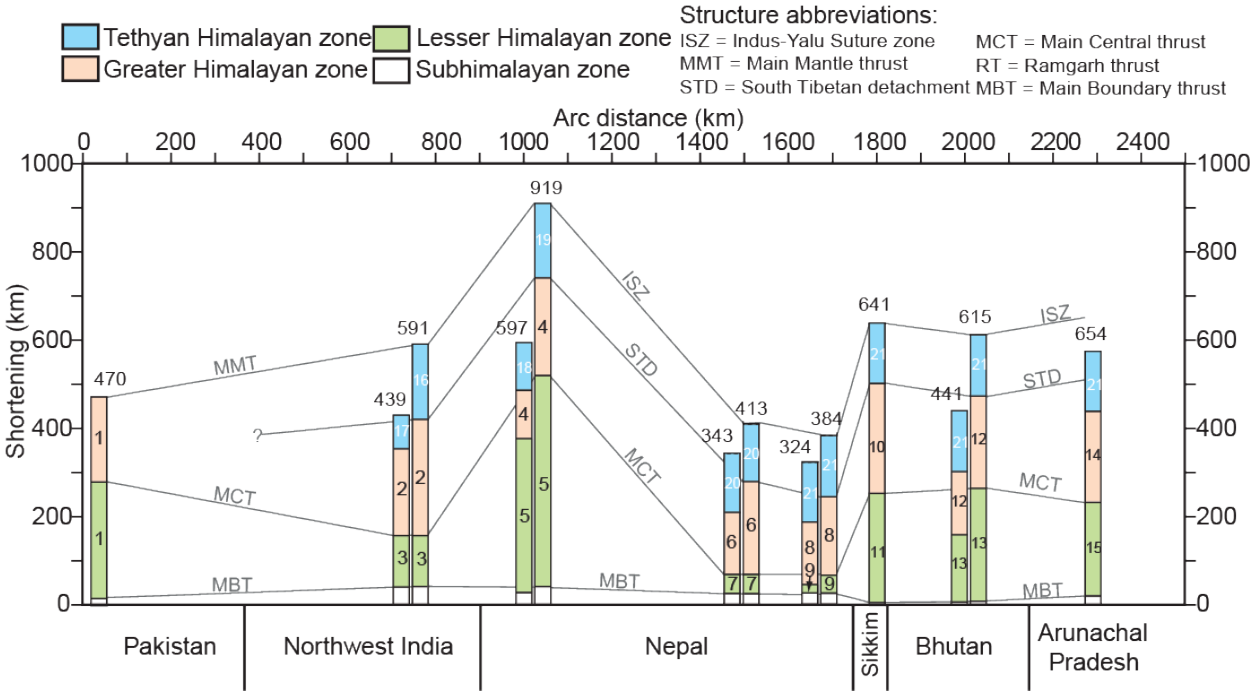

Figure 5. 3 Summary table of shortening estimates from throughout the Himalayas. After Long at al, 2011

One explanation for the variance in shortening estimates may be from a lack of data across the region and an inconstantly in the shortening estimates construction between varying research groups. Most of the research of the Himalayas is conducted in the LHS as it is more readily acceptable for field work and contains recent seismic activity. The TSS has two existing shortening estimates studies which have been used to extrapolate across the region from east to west which does not allow for analyzing of the east/west shortening differences in the TSS.

The cross section templates constructed in this study do not show a significant difference in the amount of shortening from the east to west section. This is expected as the templates are very close together and are not fully constrained based on geological structures. A more regional study is needed to determine a shortening difference in the west to east.

5.2.2 Shortening in Study Area

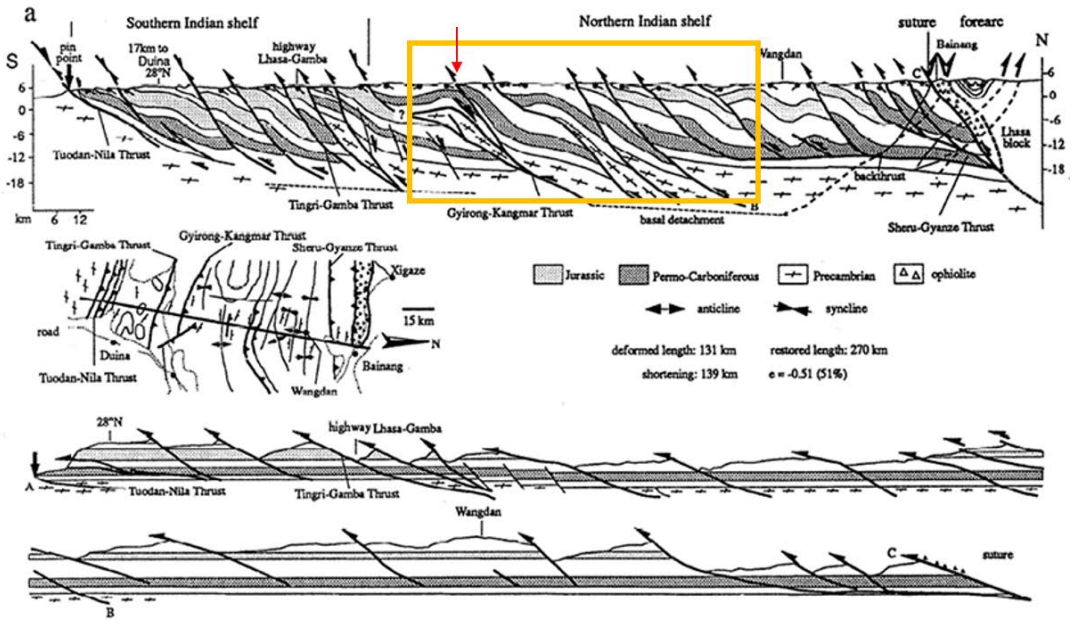

Figure 5.4. Ratschbacher et al (1994) Retro deformed cross section. Orange box shows the geographical overlap with this study. Red Arrow is debated normal or reverse fault

Currently the only existing shortening estimate of the TSS was completed by Ratschbacher et al in 1994 by hand. This research group found two shortening estimates of 133km and 139km which have a total of 67% shortening (Ratschbacher et al, 1994). The structure of these cross sections does not reflect the preliminary cross section templates created in this study with the Jiangzi map from the MOVE software. The Ratschbacher et al cross sections feature steeply dipping reverse faults with no over turned folds (figure 5.4). The 1994 study found an over all shortening percentage of 67% which is over a larger area than what is covered in this study (see orange box on figure 5.4). This study found an approximate shortening of 6% making the difference in shortening is an order of magnitude smaller in this study. This

dramatic difference in thrust dips between the 1994 study and the present 2018 study are the likely cause of this drastic difference in shortening estimates.

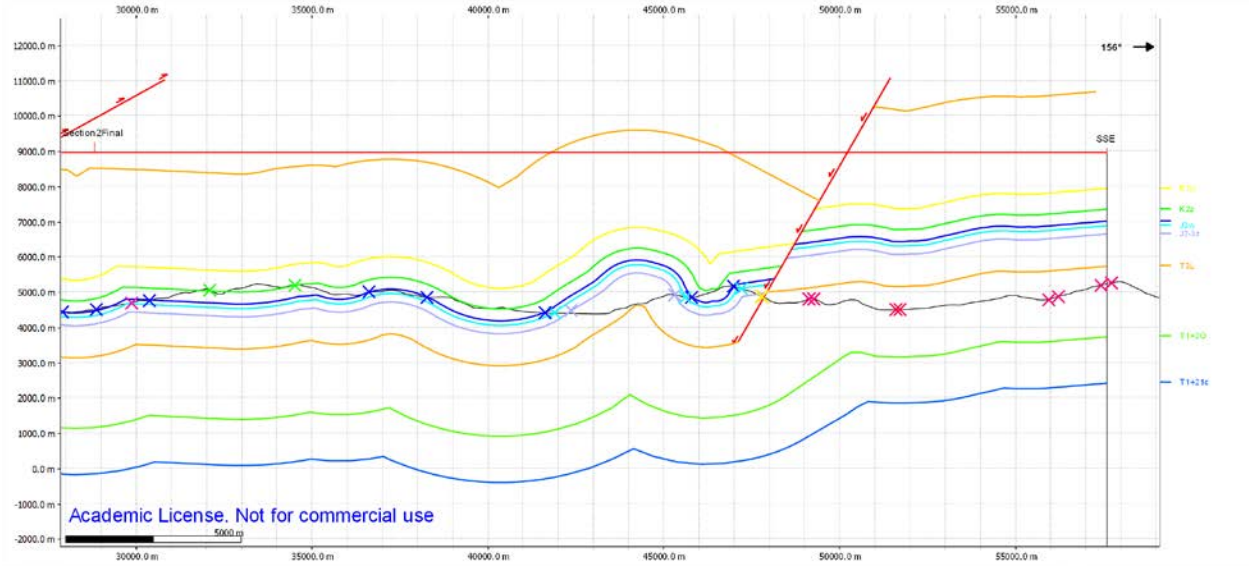

Figure 5.5 Showing the normal fault in Cross section template B which is represented as a reverse fault in figure 5.4

As well, both the Jiangzi geologic map and the Rastchbacher group indicated one of the main faults running through the section as a thrust fault. Based on the stratigraphy order the fault places younger units on top of older units indicating that it is a normal fault (Figure 5.5). Based on the fault following topographic lines on the side of a hill shown in figure 5.6, it is confirmed that the fault dips to the north. This north dipping fault with younger Jurassic layers on top of older Triassic stratigraphy confirms that the fault is normal. This discrepancy in fault movement also negatively effects the difference in the amount of shortening found between this cross section template and the Rastchbacher cross section.

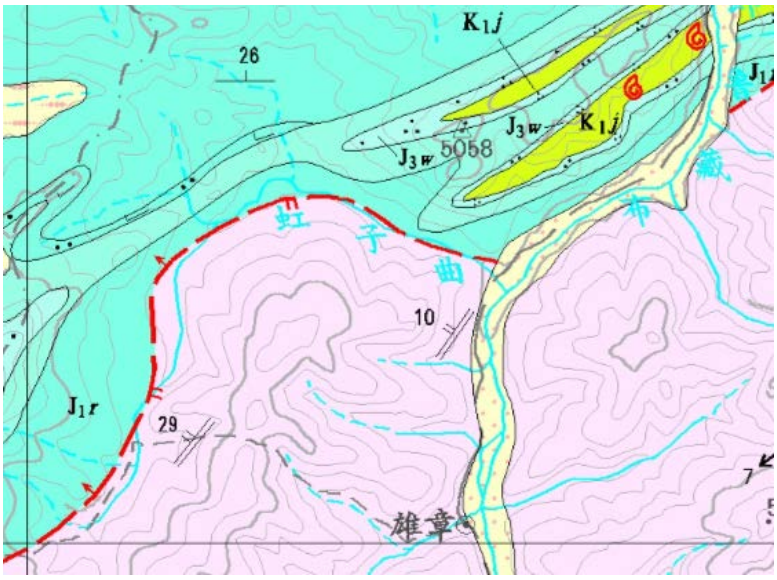

Figure 5.6. Capture of Jiangzi map showing normal fault following topographic lines of a hill, showing the fault is dipping to the north (Scale: 30 km across)

Chapter 6: Conclusions

6.1 Conclusions

There is a large need for the TSS to be studied in detail in order to provide an accurate calculation of the amount of shortening that occurred during Eocene and Oligocene. The current shortening estimates for the TSS are not accurate as they are limited to one study which is constructed by hand which is an outdated cross section balancing method and predict steep thrust faults that are not seen in other geologic maps.

Using MOVE software to make an internally consistent data set of comparable shortening estimates is an appropriate way to model the geologic structures, however this process takes a long time and should be done in conjunction with other data sources such as seismic data in order to help constrain the basal detachment.

6.2 Future Work

The cross section templates constructed in this study made an excellent starting point for more advance cross sections that will use the template as an outline for general structures. This template can be used to determine future fault prorogation studies as the cross section template can guide where faulting may occur within the syncline of a fold, in combination with more seismic structural data to constrain the basal detachment where fault propagation folds stem from. These template cross sections can also be used to guide the construction over turned folds based on the current upright folds.

Future work will include allowing for more time to construct a representative cross section and using these constructed templates to guide and advance future shortening estimates.

The two cross section templates modeled in this study can be used in the future to determine the basal detachment.

Making a cross section is an iterative process that takes many attempts to create a balance section

References

Aikman, A. B., Harrison, T. M., & Lin, D. (2008). Evidence for early (> 44 Ma) Himalayan crustal thickening, Tethyan Himalaya, southeastern Tibet. Earth and Planetary Science Letters, 274(1-2), 14-23.

Célérier, J., Harrison, T. M., Beyssac, O., Herman, F., Dunlap, W. J., & Webb, A. A. G. (2009). The Kumaun and Garwhal Lesser Himalaya, India: Part 2. Thermal and deformation histories. Geological Society of America Bulletin, 121(9-10), 1281-1297.

Chen, Z., Liu, Y., Hodges, K. V., Burchfiel, B. C., Royden, L. H., & Deng, C. (1990). The Kangmar dome: A metamorphic core complex in southern Xizang (Tibet). Science, 250(4987), 1552-1556.

Dahlen, F. A. (1990). Critical taper model of fold-and-thrust belts and accretionary wedges. Annual Review of Earth and Planetary Sciences, 18(1), 55-99.

DeCelles, P. G., Robinson, D. M., Quade, J., Ojha, T. P., Garzione, C. N., Copeland, P., & Upreti, B. N. (2001). Stratigraphy, structure, and tectonic evolution of the Himalayan fold-thrust belt in western Nepal. Tectonics, 20(4), 487-509.

Gansser A. 1964. Geology of the Himalaya. Wiley-Interscience. London.

Garzanti, E. (1999). Stratigraphy and sedimentary history of the Nepal Tethys Himalaya passive margin. Journal of Asian Earth Sciences, 17(5-6), 805-827.

Godin, L. (2003). Structural evolution of the Tethyan sedimentary sequence in the Annapurna area, central Nepal Himalaya. Journal of Asian Earth Sciences, 22(4), 307-328.

Hilley, G. E., & Strecker, M. R. (2004). Steady state erosion of critical Coulomb wedges with applications to Taiwan and the Himalaya. Journal of Geophysical Research: Solid Earth, 109(B1).

Hodges, K. V. (2000). Tectonics of the Himalaya and southern Tibet from two perspectives. Geological Society of America Bulletin, 112(3), 324-350.

Husson, L., Mugnier, J. L., Leturmy, P., & Vidal, G. (2004). Kinematics and sedimentary balance of the Sub-Himalayan zone, western Nepal.

Kawakami, T., Aoya, M., Wallis, S. R., Lee, J., Terada, K., Wang, Y., & Heizler, M. (2007). Contact metamorphism in the Malashan dome, North Himalayan gneiss domes, southern Tibet: an example of shallow extensional tectonics in the Tethys Himalaya. Journal of Metamorphic Geology, 25(8), 831-853.

Larson, K. P., & Godin, L. (2009). Kinematics of the Greater Himalayan sequence, Dhaulagiri Himal: implications for the structural framework of central Nepal. Journal of the Geological Society, 166(1), 25-43.

Lewandowski, M. (2009). Global Tectonics by Philip Kearey, Keith A. Klepeis, and Frederick J. Vine. Pure and Applied Geophysics, 166(12), 2101-2102.

Long, S., McQuarrie, N., Tobgay, T., & Grujic, D. (2011). Geometry and crustal shortening of the Himalayan fold-thrust belt, eastern and central Bhutan. Geological Society of America Bulletin, B30203.

Liu Wenchan, Li Guobiao, Wang Keyou (2002) Geological maps of the Jiangzi district sheet (1:250,000). National Geomatic Center of China (NGCC). Hebei Province Regional Geological and Mineral Survey Institute.

Mitra, G., Bhattacharyya, K., & Mukul, M. (2010). The Lesser Himalayan duplex in Sikkim: Implications for variations in Himalayan shortening. Journal of the Geological Society of India, 75(1), 289-301.

Molnar, P., & Stock, J. M. (2009). Slowing of India's convergence with Eurasia since 20 Ma and its implications for Tibetan mantle dynamics. Tectonics, 28.

Murphy, M. A., Yin, A., Kapp, P., Harrison, T. M., Manning, C. E., Ryerson, F. J., ... & Jinghui, G. (2002). Structural evolution of the Gurla Mandhata detachment system, southwest Tibet: Implications for the eastward extent of the Karakoram fault system. Geological Society of America Bulletin, 114(4), 428-447.

Murphy, M.A. and Yin, A., 2003. Structural evolution and sequence of thrusting in the Tethyan fold-thrust belt and Indus-Yalu suture zone, southwest Tibet. Geological Society of America Bulletin, 115(1), pp.21-34.

Ratschbacher, L., Frisch, W., Liu, G., & Chen, C. (1994). Distributed deformation in southern and western Tibet during and after the India-Asia collision. Journal of Geophysical Research: Solid Earth, 99(B10), 19917-19945.

Rowley, D. B. (1996). Age of initiation of collision between India and Asia: A review of stratigraphic data. Earth and Planetary Science Letters, 145(1-4), 1-13.

Tobgay, T., McQuarrie, N., Long, S., Kohn, M. J., & Corrie, S. L. (2012). The age and rate of displacement along the Main Central Thrust in the western Bhutan Himalaya. Earth and Planetary Science Letters, 319, 146-158.

Whipple, K. X., & Meade, B. J. (2004). Controls on the strength of coupling among climate, erosion, and deformation in two-sided, frictional orogenic wedges at steady state. Journal of Geophysical Research: Earth Surface, 109(F1).

Wiesmayr, G., & Grasemann, B. (2002). Eohimalayan fold and thrust belt: Implications for the geodynamic evolution of the NW-Himalaya (India). Tectonics, 21(6).

Woodward, N. B., Boyer, S. E., & Suppc, J. (1989). Balanced geological cross-sections: an essential technique in geologic research and exploration. 28th btt. Geol. Congr. Ant. Geophys. Un, Short Course in Geology, 6.

Xu, Z. Q., Dilek, Y., Yang, J. S., Liang, F. H., Liu, F., Ba, D. Z., ... & Ji, S. C. (2015). Crustal structure of the Indus–Tsangpo suture zone and its ophiolites in southern Tibet. Gondwana Research, 27(2), 507-524.